American Journal of Ophthalmology Case Reports 23 (2021) 101146

Contents lists available at ScienceDirect

American Journal of Ophthalmology Case Reports

journal homepage: www.ajocasereports.com/

Brief Report

Retinal alterations in patients with Lafora disease

Heather Heitkotter [a], Rachel E. Linderman [a], Jenna A. Cava [b], Erica N. Woertz [a], Rebecca R. Mastey [b], Phyllis Summerfelt [b], Toco Y. Chui [c,d], Richard B. Rosen [c,d], Emily J. Patterson [e], Ajoy Vincent [f], Joseph Carroll [a,b], Berge A. Minassian [g,*]

[a] Cell Biology, Neurobiology & Anatomy, Medical College of Wisconsin, Milwaukee, WI, USA
[b] Ophthalmology & Visual Sciences, Medical College of Wisconsin, Milwaukee, WI, USA
[c] Ophthalmology, New York Ear and Eye Infirmary of Mount Sinai, New York, NY, USA
[d] Ophthalmology, Icahn School of Medicine at Mount Sinai, New York, NY, USA
[e] Institute of Ophthalmology, University College London, London, UK
[f] Ophthalmology & Vision Sciences, University of Toronto, Toronto, ON, CA, USA
[g] Division of Neurology, Department of Pediatrics, University of Texas Southwestern, Dallas, TX, USA

ARTICLE INFO

Keywords:
Lafora disease
AOSLO
OCT
OCTA
RNFL
Nummular reflectivity

ABSTRACT

Purpose: Lafora disease is a genetic neurodegenerative metabolic disorder caused by insoluble polyglucosan aggregate accumulation throughout the central nervous system and body. The retina is an accessible neural tissue, which may offer alternative methods to assess neurological diseases quickly and noninvasively. In this way, noninvasive imaging may provide a means to characterize neurodegenerative disease, which enables earlier identification and diagnosis of disease and the ability to monitor disease progression. In this study, we sought to characterize the retina of individuals with Lafora disease using non-invasive retinal imaging.

Methods: One eye of three individuals with genetically confirmed Lafora disease were imaged with optical coherence tomography (OCT) and adaptive optics scanning light ophthalmoscopy (AOSLO). When possible, OCT volume and line scans were acquired to assess total retinal thickness, ganglion cell-inner plexiform layer thickness, and outer nuclear layer + Henle fiber layer thickness. OCT angiography (OCTA) scans were acquired in one subject at the macula and optic nerve head (ONH). AOSLO was used to characterize the photoreceptor mosaic and examine the retinal nerve fiber layer (RNFL).

Results: Two subjects with previous seizure activity demonstrated reduced retinal thickness, while one subject with no apparent symptoms had normal retinal thickness. All other clinical measures, as well as parafoveal cone density, were within normal range. Nummular reflectivity at the level of the RNFL was observed using AOSLO in the macula and near the ONH in all three subjects.

Conclusions: This multimodal retinal imaging approach allowed us to observe a number of retinal structural features in all three individuals. Most notably, AOSLO revealed nummular reflectivity within the inner retina of each subject. This phenotype has not been reported previously and may represent a characteristic change produced by the neurodegenerative process.

1. Introduction

Lafora progressive myoclonus epilepsy is a neurodegenerative metabolic disease caused by accumulation of insoluble polyglucosan aggregates.[1,2] These aggregates, termed Lafora bodies, build up throughout the body and central nervous system, including the neurosensory retina, and lead to progressive symptoms early in adolescence.[3] Post-mortem investigations have found retinal cell loss and Lafora bodies within and around inner retinal neurons, predominantly in the ganglion cell and inner nuclear layers.[4,5] Standard fundus examination and visual acuity testing is often unremarkable, but electroretinographic findings reveal retinal dysfunction.[6] The neural retina is accessible to noninvasive imaging and provides a window into the central nervous system. Noninvasive retinal imaging has been used to demonstrate

* Corresponding author. Division of Neurology, Department of Pediatrics, University of Texas Southwestern Medical Center, 5323 Harry Hines Blvd, Dallas, TX, USA.
E-mail address: berge.minassian@utsouthwestern.edu (B.A. Minassian).

https://doi.org/10.1016/j.ajoc.2021.101146
Received 7 October 2020; Received in revised form 4 February 2021; Accepted 12 June 2021
Available online 15 June 2021
2451-9936/© 2021 The Authors. Published by Elsevier Inc. This is an open access article under the CC BY-NC-ND license (http://creativecommons.org/licenses/by-nc-nd/4.0/).

retinal alterations in a number of neurodegenerative diseases.[7–11] Here we used spectral domain optical coherence tomography (SD-OCT) and adaptive optics scanning light ophthalmoscopy (AOSLO) in three genetically confirmed individuals with Lafora disease to look for similar retinal structural changes.

2. Materials and methods

This study followed the tenets of the Declaration of Helsinki and was approved by the Institutional Review Board at the Medical College of Wisconsin. Informed consent was obtained from all subjects, or from their legally authorized representative. Axial length was measured in each eye using an IOL Master (Carl Zeiss Meditec, Dublin, CA, USA) for scaling retinal images. One drop of phenylephrine hydrochloride (2.5%) and tropicamide (1%) was administered to one eye to dilate the pupil and suspend accommodation for imaging.

High-resolution SD-OCT volumetric (nominal 6 × 6 mm scans, 512 A-scans/B-scan, 128 B-scans) and horizontal line (nominal 6 mm) scans of the macula were acquired using a Cirrus HD-OCT device (Carl Zeiss Meditec) and/or the Bioptigen Envisu R2200 SD-OCT system (nominal 7 mm scan; Leica Microsystems, Wetzlar, Germany). Mean retinal thickness within a 6 mm radius of the foveola was calculated using Cirrus' built-in macular analysis software. Bioptigen line scans were registered and averaged as previously described.[12] The OCT line scans were then semi-automatically segmented using the Duke Optical Coherence Tomography Retinal Analysis Program (DOCTRAP) software[13] to obtain retinal thickness measurements of the ganglion cell-inner plexiform layer (GCIPL) [boundaries: bottom of the retinal nerve fiber layer (RNFL) to top of the inner nuclear layer (INL)] and the outer nuclear layer + Henle fiber layer (ONL+) [boundaries: bottom of outer plexiform layer (OPL) to top of the external limiting membrane] using custom MATLAB software (MathWorks, Natick, MA).

The foveal avascular zone (FAZ) and the vasculature surrounding the optic nerve head (ONH) were assessed in Case 3 using the AngioVue OCT-Angiography system (Optovue Inc. Fremont, CA). For each eye, multiple foveal (nominal 3 × 3 mm, 304 B-scans at 304 A-scans/B-scan) and ONH (nominal 4.5 × 4.5 mm; 400 B-scans at 400 A-scans/B-scan) scans were acquired and averaged together as previously described.[14] For FAZ measures, data were extracted from the whole retinal vasculature slab (boundaries: internal limiting membrane (ILM) to 9 μm below the OPL). For ONH scans, data were extracted from the radial peripapillary capillaries slab (boundaries: ILM to bottom of RNFL). Area and acircularity of the FAZ, segmented by a single observer (R.E.L.), as well as ONH capillary density was measured and assessed as previously described.[15–17]

Using previously described AOSLO systems,[18,19] confocal and non-confocal split-detection videos focusing on the photoreceptor layer or the RNFL were acquired at the macula and along the superior and nasal meridians. Individual videos were registered and averaged to produce single high-resolution images. The images were montaged together semi-automatically and regions of interest (150 × 150 μm) at 1° and 2° from the fovea were extracted. Cones were semi-automatically counted by a single observer (H.H.) and cone density was calculated using custom software (Translational Imaging Innovations, Inc., Hickory NC).[20] GraphPad Prism (La Jolla, CA, USA) was used for statistical analysis.

3. Results

3.1. Case 1

A 24-year-old female was diagnosed with molecularly confirmed Lafora disease after presenting with typical symptoms (compound heterozygous *EPM2A* mutations: p.Asn163Asp & p.Ala254Metfs*33). Clinical ophthalmological findings have been previously published for this patient.[6] There was overall retinal thinning at 3 and 6 mm from the fovea in both eyes (Fig. 1A). GCIPL and ONL+ thickness measurements across the macula were within the lower limits of the previously published normative range[21] (Fig. 1B). Cone density estimates at 1° (~43,600 cones/mm^2) and 2° (~36,800 cones/mm^2) from the fovea were similar to control averages[22] (average ± 2SD; 51,400 ± 13,300 cones/mm^2 and 32,500 ± 7500 cones/mm,^{2} respectively) with unremarkable and consistent cone topography (Fig. 1C). Within the RNFL near the ONH, and at the level of the ILM near the fovea, nummular reflectivity (i.e., small hyperreflective punctate structures[7]) was observed (Fig. 1D).

3.2. Case 2

A 20-year-old female was diagnosed with molecularly confirmed Lafora disease after presenting with symptoms (compound heterozygous *EPM2A* mutations: p.Arg241Ter & p.Asn163Asp). Overall retinal thinning was observed across the macula (Fig. 2A). In both eyes, six of the nine regions of the Early Treatment Diabetic Retinopathy Study (ETDRS) grid were in the lower 5th percentile for the normal distribution of retinal thickness, while one region (6 mm temporal) was in the lower 1st percentile. We were unable to acquire OCT line scans to assess GCIPL and ONL+ thickness in this patient. Parafoveal cone density estimates (Fig. 2B; 1°: ~32,800 cones/mm,^{2} 2°: ~27,000 cones/mm^2) were similar to control averages as previously published.[22] We again observed nummular reflectivity within the RNFL approximately 8° nasal to the fovea (Fig. 2C).

3.3. Case 3

A 12-year-old male, sibling of Case 2, had molecularly confirmed Lafora disease, but had not manifested clinical signs or symptoms at the time of imaging. The age of this patient was adjusted to 18 years to allow comparison to normative data on Cirrus HD-OCT device, which showed no signs of retinal thinning (Fig. 3A). GCIPL and ONL+ thickness measurements, and parafoveal cone density estimates (1°: ~50,600 cones/mm,^{2} 2°: ~36,200 cones/mm^2) were within normal limits (Fig. 3B and C).[21,22] Nummular reflectivity was observed within the RNFL approximately 5° temporal to the fovea (Fig. 3D). The FAZ area (right: 0.33 mm^2, left: 0.36 mm^2; Fig. 4A) and acircularity (right: 1.12, left: 1.19) were not significantly different in comparison to a normative database (area: 0.278 ± 0.101 mm^2; acircularity: 1.19 ± 0.095).[23] Additionally, the radial peripapillary capillary density surrounding the ONH was not significantly different from a previously published dataset,[17] though there was a general trend of increased capillary density across the whole area imaged (Fig. 4B).

4. Discussion

The retina is an extension of the central nervous system, is amenable to noninvasive imaging, and is affected by neurodegenerative processes.[24] Previous work has demonstrated that visual acuity often remains good, while electroretinographic findings reveal generalized retinal dysfunction.[6] Therefore, we sought to characterize the retinal structure of three individuals with Lafora disease using noninvasive retinal imaging (OCT and AOSLO) beyond standard fundoscopic examination. OCT is widely accessible and commonly used to evaluate RNFL and ganglion cell layer thickness to detect neurodegenerative pathology in the retina, which are used for diagnosis, assessing disease severity, and monitoring progression.[9] AOSLO provides high resolution en-face images of the retina, where individual cells in the outer retina and hyperreflective structures within the inner retina can be identified.[7,19] There were noteworthy findings observed with both imaging modalities. First, the two symptomatic patients in this series had notable retinal thinning across the macula viewed with OCT: an abnormal finding in young adults. This finding appears to be due to ganglion and bipolar cell loss, as previously suggested in histopathological reports.[4,5] Additionally, ONL+ thickness (measured on OCT) and cone density (measured on

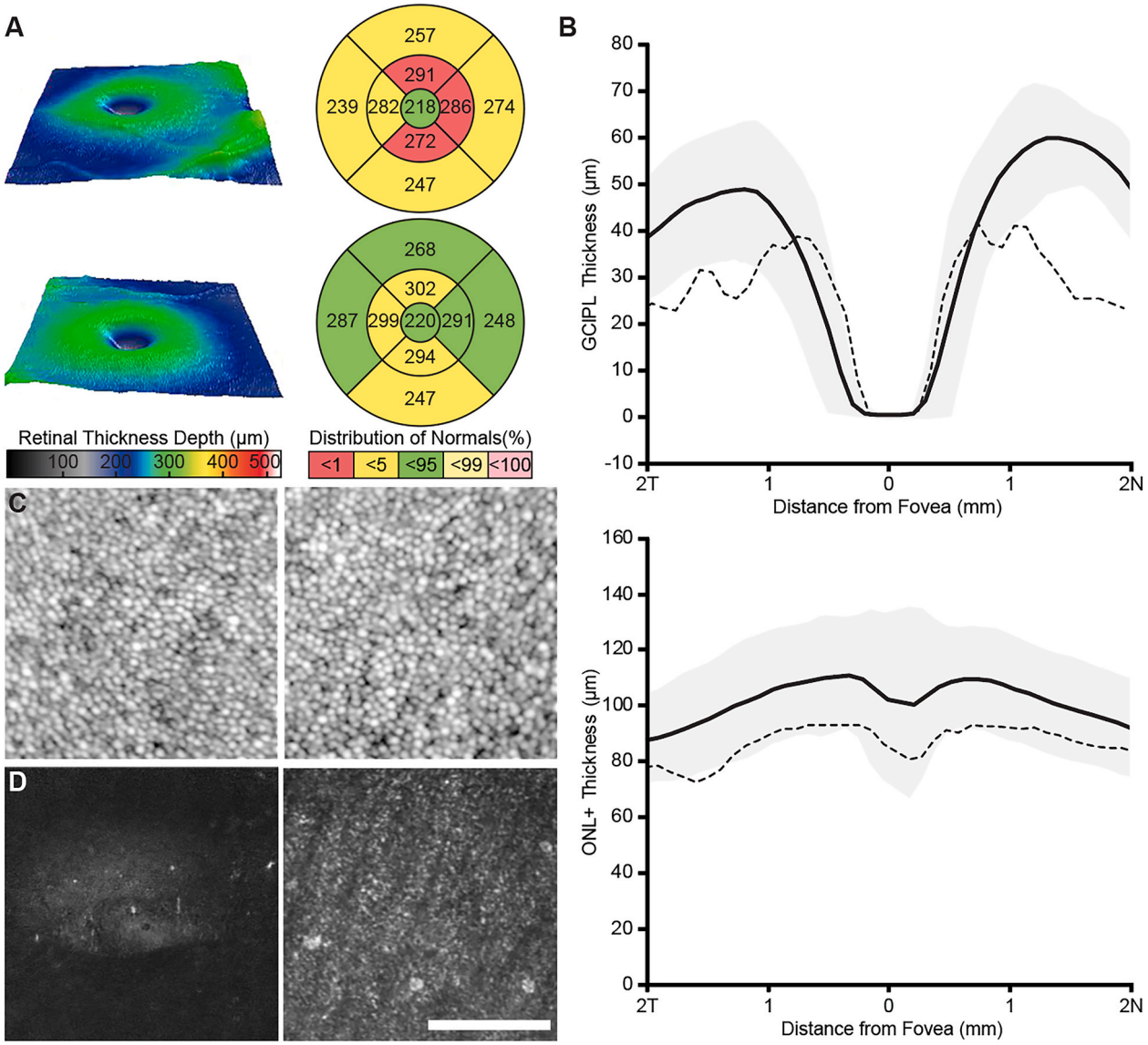

Fig. 1. Retinal imaging findings for Case 1. A) Foveal topography and Early Treatment Diabetic Retinopathy Study (ETDRS) macular thickness grids for the right (top) and left (bottom) eye acquired from Cirrus volumetric scans. This patient had overall retinal thinning in at least four regions of the ETDRS grid with overall retinal thickness at the bottom 5% of normal limits. Retinal thickness at 1 mm from the fovea in the right eye had three regions of the ETDRS grid at the bottom 1% of normal limits. B) Ganglion cell – inner plexiform layer (GCIPL, top) and outer nuclear layer + Henle fiber layer (ONL+, bottom) thickness measures across the macula, represented as a black dashed line, show retinal layer thickness measures within the lower limit of normal range (control average ± 2SD shown as black line with gray shading).[21] At 1 and 2 mm from the fovea, however, GCIPL thickness was slightly below 2 standard deviations from the control mean. C) Cone density measures at 1° (left, 43,600 cones/mm^2) and 2° (right, 36,800 cones/mm^2) from the fovea were within range of a previously published normative dataset.[22] D) Nummular reflectivity in the inner retina was found in the macula (left) at the level of the inner limiting membrane and peripherally (right) at the level of the retinal nerve fiber layer (RNFL, scale bar = 50 μm).

AOSLO) were unaffected in all three cases. These findings suggest that the outer retina is normal, or unaffected by Lafora disease, which corroborate findings from previous studies that suggest Lafora disease alters inner retinal neurons exclusively and coincides with inner retinal degeneration.[4,5] Although Lafora bodies are not visualized with the imaging modalities, it can be suggested that the changes observed in the inner retina of the affected individuals in this study are related to the neurodegenerative effects of this disease.

Most notably, nummular reflectivity – colloquially known as Gunn's dots – was observed in all three cases on AOSLO, including Case 3 (asymptomatic). The observed diameter in our patients (mean ± SD = 11.68 ± 2.4 μm) was similar to that reported in two prior studies in individuals with normal vision.[25,26] Gunn's dots can appear on the RNFL when imaged with AOSLO, but they reside somewhere within the ILM.[7] They are believed to be either a by-product of microglial phagocytosis or dead microglia that fulfilled their scavenger role in retinal pathology.[25] While nummular reflectivity can be benign, observed in younger eyes near the optic disc and in the macula of adults,[25] nummular reflectivity has been reported across several retinal and neurological conditions in areas of nerve fiber disease or loss, and may be indicative of a nonspecific neurodegenerative process.[7] The origin, function, and pathological nature of Gunn's dots remains an area of active study.[25] Further studies should be completed to determine how the presentation of Gunn's dots varies between neurodegenerative and healthy populations, as well as the relationship between the presence of Gunn's dots and inner retinal thinning.

There are certain limitations of this study. Lafora disease is a rare disorder, limiting the number of subjects available for imaging. The

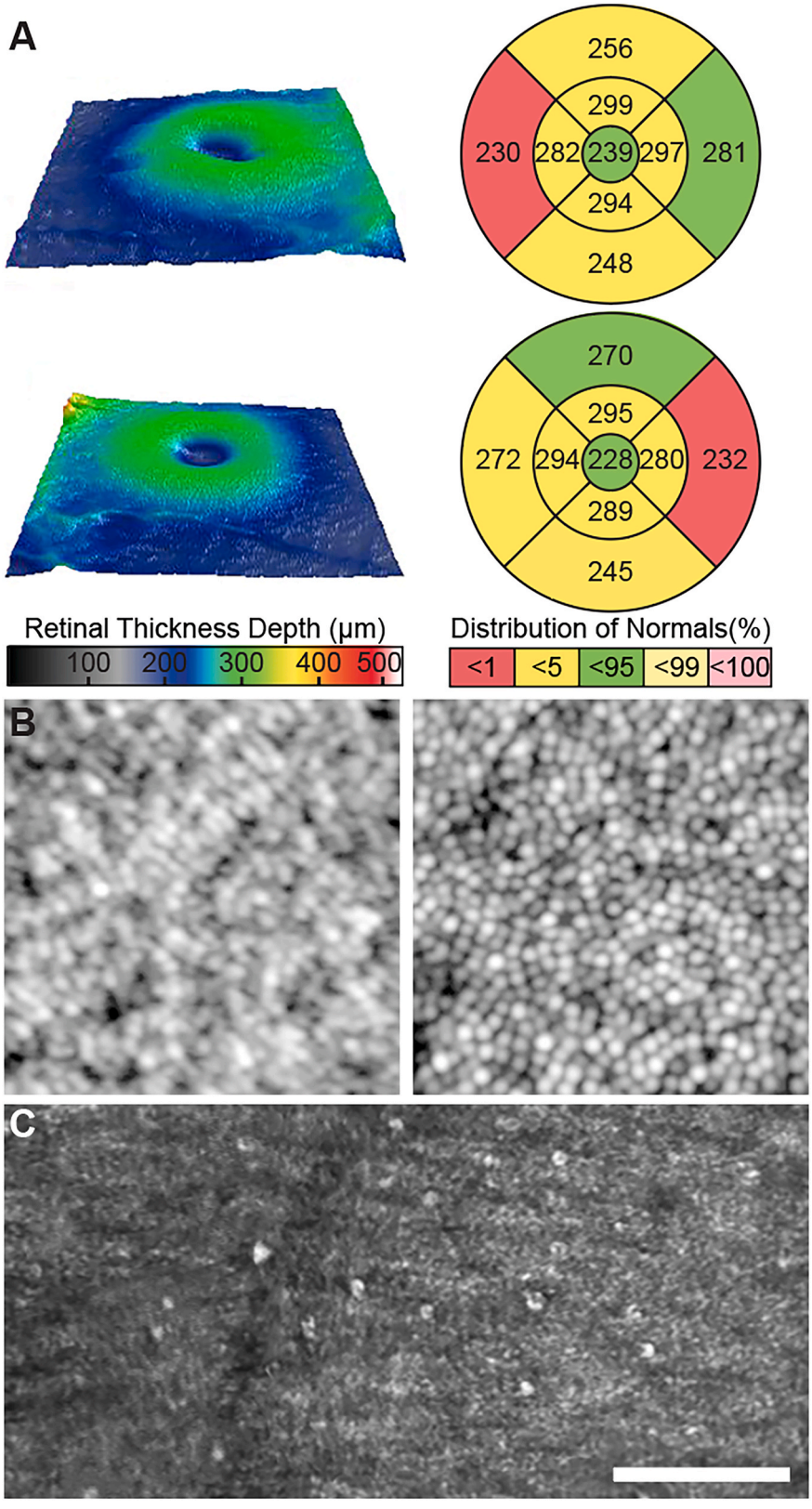

Fig. 2. Retinal imaging findings for Case 2. A) Foveal topography and ETDRS macular thickness grids for the right (top) and left (bottom) eye acquired from Cirrus volumetric scans. This patient had overall retinal thinning in seven regions of the ETDRS grids. For both eyes, retinal thickness 6 mm temporal to the fovea was in the bottom 1% of normal range. B) Cone density estimates at 1° (left, 32,800 cones/mm^2) and 2° (right, 27,000 cones/mm^2) from the fovea were within normal range when compared to a previously published dataset.[22] C) Nummular reflectivity was observed peripherally within the inner retina at the level of the RNFL (scale bar = 50 μm).

features of this disease (e.g. seizure activity and cognitive impairment) present challenges for these individuals to perform the tasks required for imaging (i.e., fixating on a target and remaining still). This can reduce the likelihood of collecting useable images, which contributed to our inability to obtain certain modalities on each individual in this study. This also presented practical limitations to the amount of time available for research testing, and we did not collect visual acuity or other visual function measures in this study. Further imaging and longitudinal follow-up within this population may clarify whether the imaging findings reported here are of clinical use in progressive

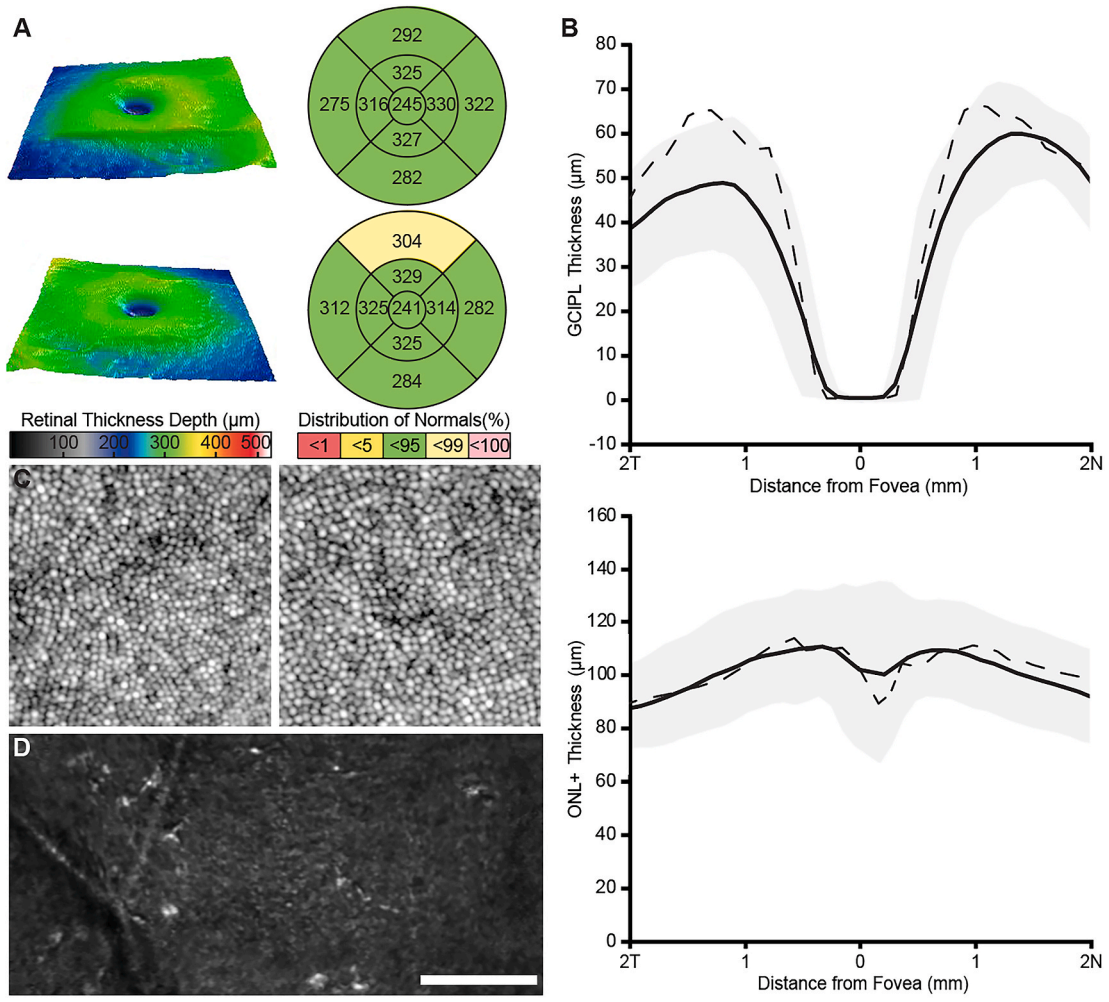

Fig. 3. Retinal imaging findings in Case 3. A) Foveal topography and ETDRS macular thickness grids for the right (top) and left (bottom) eye show normal retinal thickness acquired from Cirrus volumetric scans. The age of this patient was modified to 18 years old to obtain ETDRS measures compared to the Cirrus Normative database. B) GCIPL (top) and ONL+ (bottom) thickness measures across the macula, shown as a dashed black line, were within normal limits (control average ± 2SD shown as black line with gray shading).[21] C) Cone density estimates at 1° (left, 50,600 cones/mm^2) and 2° (right, 36,200 cones/mm^2) from the fovea were within normal range when compared to a previously published dataset.[22] D) Nummular reflectivity was found peripherally at the level of the RNFL (scale bar = 50 μm).

neurodegeneration disorders like Lafora disease. Nevertheless, our findings, in corroboration with previous reports, are consistent with the inner retina being preferentially affected by Lafora disease.[4–6] This suggests that multimodal imaging of the inner retina may be a useful tool to monitor disease progression or treatment response in patients with Lafora disease.

5. Conclusions

Consistent with previous reports,[4–6] we observed variable retinal structure in three individuals with Lafora disease when imaged with non-invasive retinal imaging techniques. A notable finding was nummular reflectivity observed within the inner retina on AOSLO in all three individuals, which may be indicative of a generalized neurodegenerative process.[7] Noninvasive retinal imaging in neurodegenerative disorders, including Lafora disease, enables identification of early disease states and provides new opportunities to monitor disease progression.[8,9]

6. Patient consent

Written consent was obtained from all subjects' legal guardian or legally authorized representative. This report does not contain any personal information that could lead to the identification of these individuals.

Funding

All funding sources for the work described are acknowledged below and had no role in study design, data analysis, or result interpretation. Funding support: C06RR016511, T32EY014537, UL1TR001436, TL1TR001437, T32GM080202, CD-CL-0617-0727-HSC, R01EY027301 and NIH P01NS097197.

Authorship

All authors attest that they meet the current ICMJI criteria for Authorship.

CRediT authorship contribution statement

Heather Heitkotter: Investigation, Software, Formal analysis, Visualization, Writing – original draft, Writing – review & editing. **Rachel E. Linderman:** Investigation, Software, Formal analysis, Visualization, Writing – review & editing. **Jenna A. Cava:** Investigation, Writing – review & editing. **Erica N. Woertz:** Investigation, Writing –

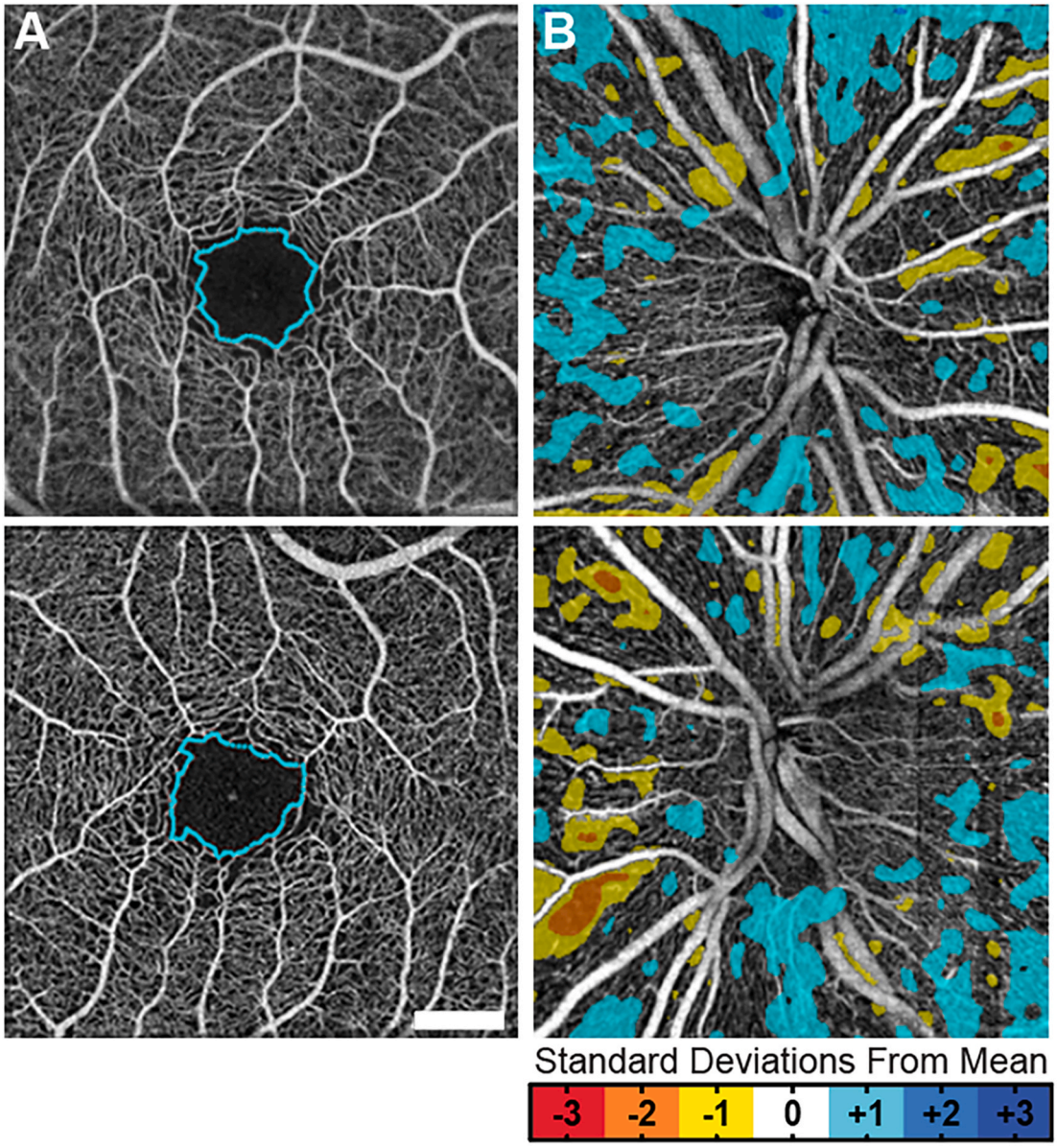

Fig. 4. Retinal vasculature findings in Case 3. A) Foveal avascular zone metrics acquired through optical coherence tomography angiography for the right (top) and left (bottom) eye are shown (scale bar = 500 μm). The foveal avascular zone, outlined in blue, was within normative range from a previously published dataset.[23] B) Standard deviation mapping of the mean capillary density surrounding the optic nerve head (ONH) of the right (top) and left (bottom) eye are shown. The ONH scans showed a slightly higher than average capillary density in both eyes but were still within normal range.[17.] (For interpretation of the references to color in this figure legend, the reader is referred to the Web version of this article.)

review & editing. **Rebecca R. Mastey:** Investigation, Writing – review & editing. **Phyllis Summerfelt:** Investigation, Project administration, Writing – review & editing. **Toco Y. Chui:** Software, Resources, Formal analysis, Visualization, Writing – review & editing. **Richard B. Rosen:** Software, Resources, Writing – review & editing. **Emily J. Patterson:** Investigation, Software, Visualization, Writing – review & editing. **Ajoy Vincent:** Conceptualization, Writing – review & editing. **Joseph Carroll:** Conceptualization, Methodology, Project administration, Funding acquisition, Resources, Supervision, Writing – review & editing. **Berge A. Minassian:** Conceptualization, Resources, Writing – review & editing.

Declaration of competing interest

Mrs. Linderman is a consultant for OptoVue. Dr. Rosen has personal financial interest in Opticology and Guardion, and is a consultant for OptoVue, Boehringer-Ingelheim, Astellas, Genentech-Roche, Nano-Retina, OD-OS, Regeneron, and Bayer. Dr. Vincent is a consultant for Adverum Biotechnologies Inc. Dr. Carroll receives financial support from AGTC and OptoVue, is a consultant for MeiraGTX, and has personal financial interest in Translational Imaging Innovations. Dr. Minassian is chief medical advisor to Taysha Gene Therapies. The following authors have no financial disclosures: H.H., J.A.C., E.N.W., R.M., P.S., T.Y.P., and E.J.P.

Acknowledgments

The authors wish to acknowledge Dr. Niamh Wynne for her contributions to this work.

References

1. Fernandez-Sanchez ME, Criado-Garcia O, Heath KE, Garcia-Fojeda B, et al. Laforin, the dual-phosphatase responsible for Lafora disease, interacts with R5 (PTG), a regulatory subunit of protein phosphatase-1 that enhances glycogen accumulation. *Hum Mol Genet*. 2003;12(23):3161–3171.
2. Nitschke F, Ahonen SJ, Nitschke S, Mitra S, et al. Lafora disease - from pathogenesis to treatment strategies. *Nat Rev Neurol*. 2018;14(10):606–617.
3. Sullivan MA, Nitschke S, Steup M, Minassian BA, et al. Pathogenesis of Lafora disease: transition of soluble glycogen to insoluble polyglucosan. *Int J Mol Sci*. 2017; 18(8):E1743.
4. Berard-Badier M, Pellissier JF, Gambarelli D, de Barsy T, et al. The retina in Lafora disease: light and electron microscopy. *Albrecht Von Graefe's Arch Clin Exp Ophthalmol*. 1980;212(3-4):285–294.
5. Yanoff M, Schwarz GA. The retinal pathology of Lafora disease: a form of glycoprotein-acid mucopolysaccharide dystrophy. *Trans Am Acad Ophthalmol Otolaryngol*. 1965;69:701–708.
6. Vincent A, Marci A, Tumber A, Koukas N, et al. Ocular phenotype and electroretinogram abnormalities in Lafora disease: a window to the brain. *Neurology*. 2018;91(3):137–139.
7. Scoles D, Higgins BP, Cooper RF, Dubis AM, et al. Microscopic inner retinal hyper-reflective phenotypes in retinal and neurologic disease. *Invest Ophthalmol Vis Sci*. 2014;55(7):4015–4029.
8. Sung MS, Choi SM, Kim J, Ha JY, et al. Inner retinal thinning as a biomarker for cognitive impairment in de novo Parkinson's disease. *Sci Rep*. 2019;9(1):11832.
9. Satue M, Obis J, Rodrigo MJ, Otin S, et al. Optical coherence tomorgraphy as a biomarker for diagnosis, progression, and prognosis of neurodegerative disease. *J Ophthalmol*. 2016;2016:8503859.
10. Biscetti L, Luchetti E, Menduno PS, Lupidi M, et al. The possible role of optical coherence tomographt (OCT) and OCT-angiography (OCTA) as new non-invasive biomarkers of prodromal Alzheimer's disease. *Alzheimers Dement*. 2020;16(S4), e042490.
11. Pellegrini M, Vagge A, Desideri LF, Bernabei F, et al. Optical coherence tomography angiography in neurodegenerative disorders. *J Clin Med*. 2020;9(6):1706.
12. Tanna H, Dubis AM, Ayub N, Tait DM, et al. Retinal imaging using commercial broadband optical coherence tomography. *Br J Ophthalmol*. 2010;94(3):372–376.
13. Chiu SJ, Li XT, Nicholas P, Toth CA, et al. Automatic segmentation of seven retinal layers in SDOCT images congruent with expert manual segmentation. *Opt Express*. 2010;18(18):19413–19428.
14. Schmidt TG, Linderman RE, Strampe MR, Chui TYP, et al. The utility of frame averaging for automated algorithms in analyzing retinal vascular biomarkers in AngioVue OCTA. *Transl Vis Sci Technol*. 2019;8(1):10.
15. Linderman R, Salmon AE, Strampe M, Russillo M, et al. Assessing the accuracy of foveal avascular zone measurements using optical coherence tomography angiography: segmentation and scaling. *Transl Vis Sci Technol*. 2017;6(3):16.
16. Linderman RE, Cava JA, Salmon AE, Chui TY, et al. Visual acuity and foveal structure in eyes with fragmented foveal avascular zones. *Ophthalmol Retina*. 2019;4 (5):535–544.
17. Pinhas A, Linderman R, Mo S, Krawitz BD, et al. A method for age-matched oct angiography deviation mapping in the assessment of disease-related changes to the radial peripapillary capillaries. *PloS One*. 2018;13(5), e0197062.
18. Dubra A, Sulai Y. Reflective afocal broadband adaptive optics scanning ophthalmoscope. *Biomed Opt Express*. 2011;2(6):1757–1768.
19. Scoles D, Sulai YN, Langlo CS, Fishman GA, et al. In vivo imaging of human cone photoreceptor inner segments. *Invest Ophthalmol Vis Sci*. 2014;55(7):4244–4251.
20. Cooper RF, Wilk MA, Tarima S, Carroll J. Evaluating descriptive metrics of the human cone mosaic. *Invest Ophthalmol Vis Sci*. 2016;57(7):2992–3001.
21. Woertz EN, Omoba BS, Dunn TM, Chiu SJ, et al. Assessing ganglion cell layer topography in human albinism using optical coherence tomography. *Invest Ophthalmol Vis Sci*. 2020;61(3):36.
22. Menghini M, Lujan BJ, Zayit-Soudry S, Syed R, et al. Correlation of outer nuclear layer thickness with cone density values in patients with retinitis pigmentosa and healthy subjects. *Invest Ophthalmol Vis Sci*. 2014;56(1):372–381.
23. Linderman RE, Muthiah MN, Omoba SB, Litts K, et al. Variability of foveal avascular zone metrics derived from optical coherence tomography angiography images. *Transl Vis Sci Technol*. 2018;7(5):20.
24. London A, Benhar I, Schwartz M. The retina as a window to the brain - from eye research to CNS disorders. *Nat Rev Neurol*. 2012;9:44–53.
25. Hammer DX, Liu Z, Cava J, Carroll J, et al. On the axial location of Gunn's dots. *Am J Ophthalmol Case Reports*. 2020.
26. Paques M, Miloudi C, Kulcsar C, Leseigneur A, et al. High-resolution imaging of gunn's dots. *Retina*. 2015;35(1):120–124.